

## Performance characteristics and reliability assessment of self-excited induction generator for wind power generation

Varshney, Lokesh; Vardhan, Aanchal Singh S.; Vardhan, Akanksha Singh S.; Kumar, Sachin; Saket, R. K.; Sanjeevikumar, P.

*Published in:*  
IET Renewable Power Generation

*DOI (link to publication from Publisher):*  
[10.1049/rpg2.12116](https://doi.org/10.1049/rpg2.12116)

*Creative Commons License*  
CC BY 4.0

*Publication date:*  
2021

*Document Version*  
Publisher's PDF, also known as Version of record

[Link to publication from Aalborg University](#)

*Citation for published version (APA):*  
Varshney, L., Vardhan, A. S. S., Vardhan, A. S. S., Kumar, S., Saket, R. K., & Sanjeevikumar, P. (2021). Performance characteristics and reliability assessment of self-excited induction generator for wind power generation. *IET Renewable Power Generation*, 15(9), 1927-1942. <https://doi.org/10.1049/rpg2.12116>

### General rights

Copyright and moral rights for the publications made accessible in the public portal are retained by the authors and/or other copyright owners and it is a condition of accessing publications that users recognise and abide by the legal requirements associated with these rights.

- Users may download and print one copy of any publication from the public portal for the purpose of private study or research.
- You may not further distribute the material or use it for any profit-making activity or commercial gain
- You may freely distribute the URL identifying the publication in the public portal -



### Take down policy

If you believe that this document breaches copyright please contact us at [vbn@aub.aau.dk](mailto:vbn@aub.aau.dk) providing details, and we will remove access to the work immediately and investigate your claim.



## ORIGINAL RESEARCH PAPER

# Performance characteristics and reliability assessment of self-excited induction generator for wind power generation

Lokesh Varshney<sup>1</sup> | Aanchal Singh S. Vardhan<sup>2</sup> | Akanksha Singh S. Vardhan<sup>2</sup> |  
Sachin Kumar<sup>3</sup>  | R.K. Saket<sup>3</sup>  | P. Sanjeevikumar<sup>4</sup>

<sup>1</sup> Department of Electrical Engineering, Galgotias University, Greater Noida, Uttar Pradesh, India

<sup>2</sup> Department of Electrical Engineering, Shri G.S. Institute of Technology and Science, Indore, Madhya Pradesh, India

<sup>3</sup> Department of Electrical Engineering, Indian Institute of Technology (BHU), Varanasi, Uttar Pradesh, India

<sup>4</sup> Center for Bioenergy and Green Engineering, Department of Energy Technology, Aalborg University, Esbjerg, Denmark

**Correspondence**

R. K. Saket, Department of Electrical Engineering, Indian Institute of Technology (BHU), Varanasi, Uttar Pradesh, India.  
Email:

**Abstract**

The paper presents the performance analysis-based reliability estimation of a self-excited induction generator (SEIG) using the Monte-Carlo simulation (MCS) method with data obtained from a self-excited induction motor operating as a generator. The global acceptance of a SEIG depends on its capability to improve the system's poor voltage regulation and frequency regulation. In the grid-connected induction generator, the magnetizing current is drawn from the grid, making the grid weak. In contrast, in the SEIG stand-alone operation, an external capacitor arrangement is implemented to render the reactive power support. This capacitor arrangement is connected across the stator terminals during the stand-alone configuration of SEIG. The capacitor serves two purposes, which include voltage build-up and power factor improvement. Therefore, the paper deals with obtaining the minimum capacitor value required for SEIG excitation in isolated mode applications, including stand-alone wind power generation. The SEIG performance characteristics have been evaluated for different SEIG parameters. The simulation and experimental results are then compared and found satisfactory. Then, SEIG reliability is estimated considering the MCS method utilizing SEIG excitation's failure and success rates during experimental work in the laboratory. Finally, the SEIG reliability evaluation is performed considering different wind speeds.

## 1 | INTRODUCTION

The performance of self-excited, induction generator (SEIG) depends on many factors including machine parameters, type of loading, rotor speed, voltage regulation (VR), frequency regulation (FR) and methods to implement the excitation system. The prime mover speed, value of the capacitance, impedance load, etc., depends on SEIG frequency and voltage. The SEIG performance badly suffers from the poor voltage and frequency drop due to loss in residual magnetism (RM). This loss phenomenon is briefly explained in subsequent sections of this paper. Furthermore, it is also observed that most of the previous theoretical and experimental researches were performed to improve the poor VR and FR for enhancing the performance of SEIG. In previous studies, the performance characteristics,

VR and FR, construction and design, capacitance requirements, steady-state (SS) and dynamic performances of SEIG were described. The aforementioned parameters are well discussed in the present research work.

To achieve the optimum SEIG performance, especially in the SS and transient conditions [1–3], the combinational arrangement of speed, shunt, and serial capacitances is done, and the ideal VR and FR values are obtained [4]. Recently, authors of [5] have explained the experimental analysis of an isolated three-phase SEIG in SS to provide a regulated voltage in an economical manner. The voltage at the SEIG terminal and system frequency is unknown in a far-flung power system. The frequency and voltage have to be evaluated at a constant capacitance value, speed and load. To harness the maximum wind energy under wind speed variation, a suitable pole changing

method of SEIG is described in [6]. Authors in [7] have presented an approach to predict required self-excitation capacitor value of SEIG. The wind turbine driven parallel operated SEIG performance under unbalanced loads is described in [8]. The authors present these performance characteristics for a given SEIG and the characteristics are validated on an experimental laboratory setup.

The SEIG performance under unbalanced conditions replicates power loss, extra heating, insulation failure due to winding stress and shaft vibrations [9]. Authors in [10] have presented the transient performance analysis of SEIG considering short-shunt configuration. The voltage erection in SEIG at the rated speed is critical due to the switching of the 3- $\phi$  capacitor hub at no-load. Authors in [11] have introduced the transient analyses under the voltage buildup process [12] of a stand-alone SEIG by switching-off (i) single capacitor for excitation, and (ii) multiple capacitors for excitation. It is observed that the SEIG constantly maintains self-excitation and produces terminal voltage sufficiently on the two phases when any one of the phase capacitors is out of service. The SEIG with a long shunt configuration is having undesirable fluctuations while the SEIG with a short-shunt configuration gives a better VR [13]. The transient performance of a series-compensated 3- $\phi$  SEIG with a dynamic load is described in [14]. Therefore, the voltage formation and self-excitation processes for an available SEIG can be defined mathematically with experimental validation, as explained in this work.

Furthermore, the technical implementation and design aspects of an Electronic Load Controllers (ELC) for optimum voltage and frequency of a three-phase SEIG driven by unregulated turbine feeding variable loads in remote locations are proposed in [15, 16]. This controller is proposed for a stand-alone application of SEIG. Besides of using costly speed-governor during electrical power generation, the load controller may be implemented to regulate the frequency of SEIG. The speed and frequency are maintained at a constant level using a load controller that sinks the excess power of the SEIG into the resistive load [9]. Authors in [17] has proposed a method in which the magnetizing reactance and capacitance values are needed for self-excitation phenomena in SEIG to improve the performance in terms of voltage, frequency, power factor, active and reactive power and other parameters.

It is well known that for Volt–Ampere Reactive (VAR) compensation, Flexible Alternating Current Transmission System (FACTS) device is used in an electrical power system. Integration of Static Compensator (STATCOM) and variable frequency drive in [18] is presented to control the SEIG voltage and frequency, respectively. A current synchronous detection method using STATCOM is proposed in [19] and Dynamic Static Compensator (DSTATCOM) in [20] for SEIG voltage and frequency management. A proportional-resonant control method using DSTATCOM for VR of three-phase/one-phase SEIG driven by variable micro-hydro turbine is proposed in [21, 22].

The research work explained above mainly focuses on VR and FR due to the uncertainties in voltage and frequency in wind turbine driven SEIG. Therefore, the performance analysis

of SEIG as an isolated generation mode is necessary. The self-excitation methodology in [23] presents that by using a capacitor hub externally in an isolated mode, the induction machine can be operated as a Induction Generator (IG) [24]. The required magnetization current for SEIG is provided by the following excitation methods [25]:

- (i) By fixed capacitor,
- (ii) By switched capacitor,
- (iii) By controlled capacitors and
- (iv) With controlled reactance and capacitors.

Security and adequacy are the main attributes in the reliability evaluation (RE) of the electrical generation system [26]. The RE is focused only on the generation system adequacy [27–32]. In addition, the literature describes the SEIG generation RE method. It also provides a detail of the success and failure probability of RM in the SEIG. The reliability indices like Mean Time To Failure (MTTF), Mean Time Between Failure (MTBF) and Mean Time To Repair (MTTR) are commonly used in this process and are evaluated experimentally. The comparison of present work with previously published work is described in Table 1. The main contributions are highlighted as follows:

- The performance of a laboratory-based SEIG is evaluated at variable load impedance ( $Z_L$ ) and variable rotor speed.
- The requirement of minimum capacitor value for the SEIG is calculated mathematically with experimental verification of results. The results show that the method is effective to get better performances of a given SEIG by selecting the optimal excitation capacitance.
- The probabilistic RE is performed for the SEIG used in the experimental setup. The common attributes in RE of any equipment include success probability, adequate function, the period of time and operating conditions.
- The reliability functions are evaluated for RM failures and safe operational regions of 3- $\phi$  squirrel cage induction machine operated as SEIG in remote areas, where arrangements for the restoration of RM are not available.
- Reliability analysis of SEIG under different wind speeds is performed, and the impacts on the SEIG reliability are studied.

Furthermore, the paper has been organized as follows. In Section 2, a detailed description of SEIG is described. The self-excitation process, voltage build-up process and the optimal value of the capacitor required at a particular rotor speed are briefly discussed in Section 2. Section 3 includes the calculations of  $X_m$  and  $f$  using the two equations to obtain the air gap voltage. In this section, constant terminal voltage characteristics and critical characteristics are also graphically presented. The reliability estimation of RM in the SEIG rotor core using a probability distribution approach and a Monte-Carlo method is implemented and discussed for success and failure probability evaluation in Section 4. The SEIG circuit model, its variable and constant parameters, its third-order equation with coefficients are expressed, discussed and determined in

**TABLE 1** Comparison to previously accomplished work

Reference	Previously accomplished work	Present work
[5]	The experimental analysis of an isolated 3- $\phi$ SEIG in steady state to provide a well-regulated voltage in an economical manner	The MATLAB simulation results are verified by experimental results in an economical manner
[6]	Harness the maximum wind energy under wind speed variation using a suitable pole changing of SEIG.	Applicable to harness maximum wind energy at variable wind speed only using a capacitor hub in the remote area for stand-alone operation
[7, 17]	To predict the required self-excitation capacitor value of SEIG	To obtain the initial RM a proper excitation capacitor value is obtained using simulation and verified by laboratory experiment
[9, 10]	Wind turbine driven SEIG performance characteristics under unbalanced loads	SEIG performance characteristics are obtained and verified for unbalanced loads
[11, 14]	Transient analysis undervoltage build-up process of a stand-alone SEIG by switching off single and multiple capacitors	Only a 3- $\phi$ capacitor hub is implemented for initial RM and voltage build-up
[13]	Short-shunt configuration for better voltage regulation.	No extra configuration is implemented for obtaining a better voltage regulation
[15, 16, 18–22]	Electronic load controller, STATCOM and other FACTS devices are implemented for VAR compensation and voltage and frequency regulation.	VAR compensation, voltage and frequency regulation may be achieved economically
	No work is done on reliability assessment	Reliability assessment is accomplished

Section 5. Also, the magnetization and typical characteristics of the SEIG with experimental results; and graphical representation of different reliability-related functions and the SEIG reliability at different wind speeds are evaluated in this section. The conclusions and future scopes are presented in Section 6. At the end of the work, some related data are provided in the Appendix.

## 2 | SEIG: AN OVERVIEW

The IG has vast applications due to its low cost, mechanical, and electrical simplicity compared to other generators. The main feature of IG is output power ( $P_O$ ) generation at varying speeds [9, 33]. This is a feature that enables the IG operation in stand-alone mode to supply widely distributed and remote areas. IG in isolated mode is needed where the expansion of the is not economically feasible. Also, an isolated mode of IG is utilized in combination with the synchronous generator when localized power demand is raised. The real power demand of the grid is fulfilled when IG is in grid-connected mode.

The no-load test investigates the self-excitation phenomenon in SEIG. Also, the capacitor calculated limits are compulsory for excitation in SEIG. The magnetization curve is determined. In this test curve, the circuit parameters of the induction machine are considered to be constant except magnetizing inductance ( $X_m$ ). The terminal voltage of SEIG at no-load is the meeting point of the magnetizing curve and capacitive load line. In an IG, the voltage level is determined by an external capacitor which is capable of supplying the magnetizing current ( $I_m$ ). The shaft speed, RM and the reduced permeability are the other parameters at lower magnetization that affect the self-excitation process in SEIG.

An IG gets excitation either from an external capacitor hub or an electrical power grid. In the grid-connected mode of operation, the IG draws reactive power from the grid, creating electrical stress on the power grid. A capacitor hub connected across the stator terminals supplies reactive power in an isolated mode of operation. This process is termed as capacitive self-excitation phenomena. Hence, an IG is termed as a ‘SEIG’. The minimum RM must be available in the SEIG rotor as similar to the DC generator. So it is desirable to maintain an optimum RM for SEIG excitation. A small terminal voltage due to the minimum RM is available at the beginning of an IG. A capacitor current ( $I_C$ ) flows due to this terminal voltage, which helps in the voltage build-up process. Hence, an external capacitor is connected to obtain the desired voltage level in an IG, which supplies the magnetizing current [33].

### 2.1 | Effect of capacitance on rotor speed of SEIG

The minimum ( $C_{\min}$ ) and maximum ( $C_{\max}$ ) values of the capacitor are needed for self-excitation of a 3- $\phi$  IG. The current model and flux model are used to obtain the  $C_{\min}$  and  $C_{\max}$  values, respectively. It is not desirable to obtain the  $C_{\max}$  value because of voltage rating compatibility and cost-effectiveness. Furthermore, the current flowing at  $C_{\max}$  exceeds the rated stator current.

The work illustrates the characteristics among speed, capacitance and the load of the SEIG, which are obtained with continuous variation in load without loss of excitation. The minimum and maximum speeds are needed for self-excited wind driven IG under loading conditions. An analytical approach is used for graphical representation of the  $C_{\min}$  and  $C_{\max}$  values for establishing the self-excitation at a defined rotor speed.

## 2.2 | RM: Loss and retrieval

To avoid the disturbance in the RM, the following four procedures are useful and can be adapted for the retrieval of magnetism:

- (i) Use of an AC excitation system for operating the induction machine as a motor for up to 15 min;
- (ii) By implementing the terminal capacitors, which are completely charged up to the voltage rating of the machine. The discharge current of the capacitor is sufficient for the self-excitation of the machine;
- (iii) By raising the rotor speed of the machine above the rated causes an increment in speed at lower magnetization, thereby creating self-excitation at rotor maximum speed and
- (iv) By connecting a DC battery over the machine terminals for 10–15 min when the machine is in rest.

As per the above-mentioned procedures for the grid-connected operation, procedure (i) is better in comparison to other procedures while for the islanded operation, procedure (iii) is commonly used. In this research, procedure (ii) is implemented due to excitation capacitor availability and better VAR compensation during the isolated mode of operation.

Generation based on SEIG is mainly dependent on (i) speed of the shaft, (ii) RM of the rotor core, (iii) reduction in permeability value at low magnetization and (iv) the capacitor value, which is connected to the machine. If one of them is weak, the loss of excitation occurs. Sometimes, under the condition of excitation loss, the SEIG loses its RM. The present work describes theoretically and experimentally all of the above factors in SEIG performance analysis.

## 3 | PERFORMANCE CHARACTERISTICS OF SEIG

The performance characteristics of the isolated SEIG are somewhat complex in comparison to the grid-connected IG. In SEIG, the voltage and frequency also depend on capacitor and load impedance values in contrast to the rotor speed of grid-connected IG. The loop impedance methodology [10] and the nodal admittance methodology are used in examining the circuit. These approaches are applied where two simultaneous non-linear equations are available. The SEIG mathematical expressions are given in terms of  $X_m$  and  $f$ . The expressions can be solved by distinguishing the real and imaginary components of the equivalent circuit impedance. After getting the numerical values of  $X_m$  and  $f$ , the determination of the generator's SS performance is done using its equivalent circuit and magnetization curve. The detailed derivation is not required for this simple approach to solving the non-linear equations [34]. Thus, it is difficult to define the performance of the SEIG. The simulation results are then compared to the experimental results. The experimental circuit model and experimental setup are shown in Figures 1(a) and (b), respectively. The experimental induction

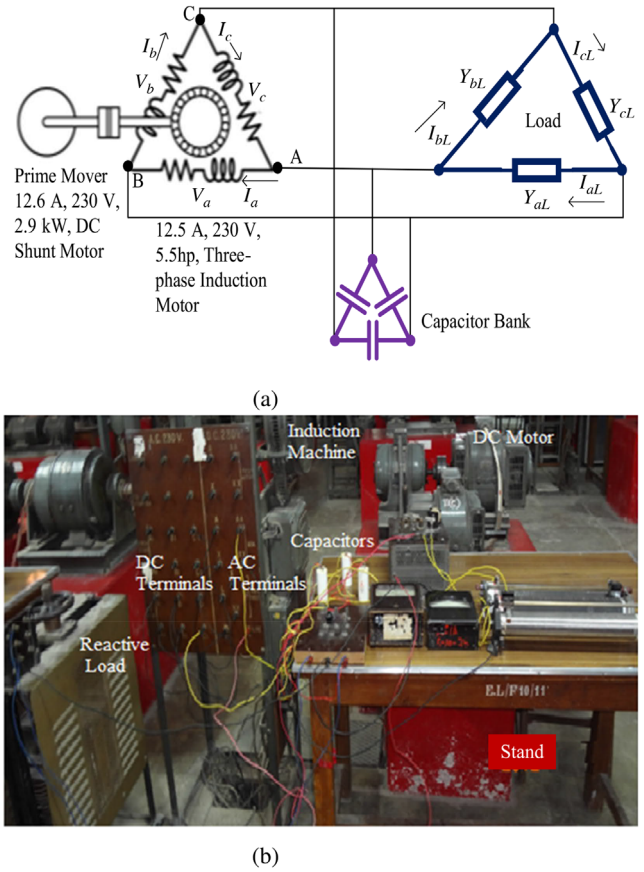


**FIGURE 1** (a) The analogous schematic of a 3- $\phi$  SEIG with load impedance and capacitor hub; (b) Experimental setup

machine's parameters and rating are given as follows:

Three-phase, four-pole, 50 Hz, 230 V, 12.5 A,  $R_s = 3 \Omega$ ,  $R_r = 1.58 \Omega$ ;  $X_s = X_r = 1.6 \Omega$ ,  $R_c = 1485.27 \Omega$ . The following assumptions are made for the SS analysis:

- (i) The generator parameters are considered as constant except  $X_m$ ,
- (ii) Stator and rotor leakage reactance are presumed to be identical and
- (iii) The harmonic contents of the current waveform and induced Electromotive Force waveform are neglected.

## 3.1 | SEIG circuit modelling

In Appendix A, Figures A1(a) and (b) describe the per-phase SS analogous circuit of a SEIG with  $Z_L$  and the equivalent circuit of nodal admittance approach, respectively. In this figure,  $R_s$ ,  $R_r$ ,  $R_c$  and  $R_L$  are stator, rotor, core and load resistances, respectively.  $X_s$ ,  $X_r$ ,  $X_m$ ,  $X_c$  and  $X_L$  represent the reactances of the stator, rotor, magnetizing, excitation capacitor, and load, respectively.  $V$  and  $f$  signify the speed and frequency in pu, respectively. The variable parameters in this analogous circuit are  $X_c$ ,  $f$ ,  $V$  and  $Z_L$ . Thus, five parameters including  $X_m$ ,  $X_c$ ,  $f$ ,  $V$  and  $X_L$  are adjustable in the per-phase SS study of a SEIG [34, 35].



The normalization is done at the base frequency by dividing all the circuit parameters including  $V$  by the frequency  $f$  for the analogous circuit. A constant load power factor  $\angle\theta$  is assumed at the base frequency to obtain the  $Z_L$  which is given in (1). Thus, the equivalent circuit is shown in Figure A1(a) have variables including  $X_m$ ,  $X_c$ ,  $f$ ,  $V$  and  $Z_L$ . All the variables must be described effectively to obtain the SEIG performance.

$$Z_L = |Z_L| \angle\theta = (R_L + jX_L), \quad (1)$$

where  $|Z_L|$  is the modulus of  $Z_L$ .

### 3.2 | Problem statement: SEIG performance and RE

The self-excitation importance in an induction machine is briefly described in the previous sections. This excitation occurs when an optimal value of the capacitor is connected across the stator terminals. The SEIG  $f$  and  $X_m$  vary with the load even at constant rotor speed. Therefore, the following steps in SEIG are considered for SS analysis.

Step I: Obtain machine parameters with rotor speed, excitation capacitor value and  $Z_L$ .

Step II: Determine the values of  $f$  and  $X_m$ , which result in the accurate balancing of active and reactive power across the air gap.

The parameters' values are the main reason for the sluggish performance of the SEIG. The parameter values are determined during the design of SEIG. The parameters of the machine were optimized when the machine was operating in the motoring mode instead of generating mode.

The induction machine may work in two parts, namely, the unsaturated or linear part and the saturated or non-linear part of the hysteresis or saturation characteristic. But it is not acceptable to run an induction machine in the saturated part. This reduces the iron core's relative permeability and raises the magnetomotive force needed to run the machine. Also, the machine working in the linear part does not wholly exploit the effectiveness of the iron. Therefore, this concept is not prudent. This results in the most acceptable working set of points for an induction machine, which is known as the knee of the machine characteristic. These points exaggerate the utilization of the iron core while lessening its saturation. To utilize the induction machine as an IG, the voltage at the stator terminals of the machine is raised until the magnetic circuit reaches the saturation stage. Finally, SEIG works after the knee point of saturation characteristic.

The soft or malleable magnetic substance is utilized in the rotor core of the Induction Motor (IM), which has the narrower hysteresis loop. Alternatively, hard or strong magnetic substances are utilized in the rotor core of the designed SEIG, which has a wider hysteresis loop. Accordingly, the hysteresis effect is in consideration in the machine's rotor. Thus, the SEIG rotor core has sufficient RM, which is needed for SEIG excitation. In this situation, the issue related to loss of excitation may exist while using the IM as SEIG. Therefore, operating

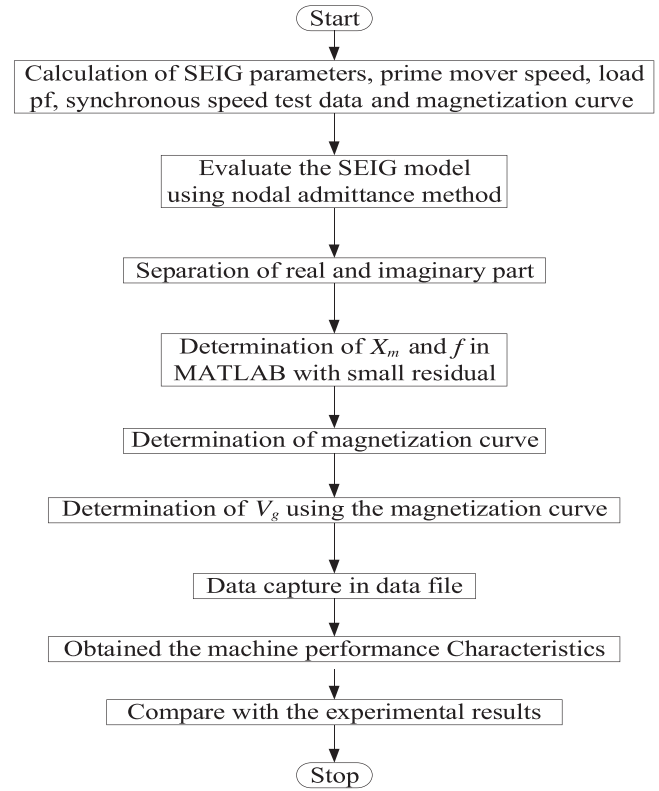


FIGURE 2 Algorithm for SEIG performance characteristics

an induction machine as a SEIG is extremely popular. Thus, the reliability assessment of the machine rotor (run as SEIG) is demanded, as discussed in Section 4. The overall performance evaluation algorithm of a SEIG is given in Figure 2.

## 4 | RE OF SEIG

The reliability calculations are segregated into two models: the deterministic model and the probabilistic model. A significant drawback of these models is that they do not consider the stochasticity of the electrical system. Probabilistic models can yield relevant instruction utilized in the study and resource planning and allotment. Two modes utilize the probabilistic calculation. The analytical methods serve as the system by numerical models and employ direct analytical solutions to assess reliability indices from the designed model. As for the Monte-Carlo method, reliability indices are determined by simulating the exact random behaviour of the electrical system. The technique for reliability and accuracy assessment is conferred in the later subsections.

The parameters that are typically accompanied by reliability and safety assessment are represented by probability and/or possibility distributions. This can easily be realized by studying that all components of a given type and construction must be in working condition. All will not be failed after the same working point but may fail at a distinct point in times. In all practical cases, the relevant probability distribution can be deduced from sample analysis or statistics of data collection. This

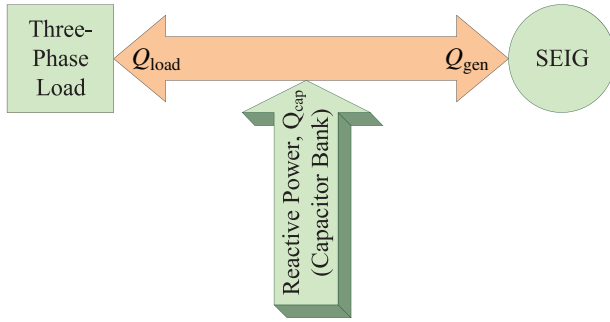


**FIGURE 3** Reactive power distribution in an isolated SEIG system

analysis scheme is correlated with the working of the components, devices, and/or systems.

#### 4.1 | Monte-Carlo simulation

The reliability-related indicators are assessed using direct analytic or stochastic techniques. So, to deal with the actual engineering problems, the stochastic simulation technique is suitable. Statistics or other basic calculations are employed in the analytical technique to access the indices. And the reliability indices are evaluated by simulation technique, which simulates the actual process and irregular behaviour of the system. Monte-Carlo method estimates the probability and reliability indices by simulating the outputs several times.

The simulation technique, thus, deals with the problem as a set of a real-time experiment performed within simulation time. These real experiment results show the following points:

- (i) Several experiments provide a better measure of the success probability and failure probability,
- (ii) The values of both the probabilities are obtained for the number of real experiments,
- (iii) The mean values of the probabilities are not a proper estimate of the real value;
- (iv) The real value is sometimes given the experiments, but this would not generally be established and
- (v) On the repetition of the process, the sequence outcomes provide a specific pattern of probability values.

#### 4.2 | Problems related to SEIG failure due to excitation

The authors have developed a SEIG using an IM. This SEIG contains an excitation capacitor of an appropriate value. The reliability of the self-excitation must be extremely large by raising the excitation capacitor value. The implementation of the excitation capacitor in SEIG generates  $P$  and  $Q$ . These powers are delivered to the IG for self-excitation and the connected impedance load, as shown in Figure 3.

At constant shaft speed and fixed capacitor value, if the  $Z_L$  decreases little from the threshold value of  $Q_L$  and  $Q_E$  shifts to  $Q_L$ , which results in a dip in the terminal voltage. To pre-

vent the dip in the voltage, either the value of the capacitor can be increased, or the shaft speed can be increased, or both can be increased. However, the rotor core's RM and permeability may not be modified during the performing stage of the SEIG. The terminal voltage drops and load disconnects if the capacitor is not at its acceptable value and the shaft speed is not built up. Occasionally, the failure of RM occurs. This issue of the experimental SEIG has been dealt with for reliability and security assessments.

The evaluation of SEIG's reliability is performed for loss of the RM at a minimum value of the capacitor and constant speed. The second cause of loss of excitation failure in SEIG is the insufficient shaft speed for fixed capacitor value and constant  $Z_L$ . Reliability has been evaluated in two forms, one is based on decreasing  $Z_L$ , and the other is based on decreasing shaft speed from the critical value, which is described in the present work.

#### 4.3 | Reliability assessment of the SEIG

Several experiments are performed on SEIG with a minimum value of excitation capacitor. Refer Appendix 'A' for IM parameters and ratings and per-phase equivalent parameters' circuit of IM. Reliability quantification is an important aspect of the reliability assessment of the generation system. The values of parameters obtained from the measurement are used to quantify the reliability of a generation system and are given by various reliability indices. These reliability indices are exploited to assess the reliability performance of a generation system. Some pre-determined minimum reliability standards, alternative designs, identified weak spots, and identified ways for correction in the generation system are considered in this work. These are considered for integration with costs and performance analysis in decision making.

The numbers of indices have been introduced in reliability theory to facilitate reliability predictions and others to fit various applications quite generally. All of these indices can be classified into the following categories: (i) Probability distribution function,  $f(t)$ ; (ii) Cumulative distribution function,  $F(t)$ ; (iii) Survivor function,  $f_s(t)$ ; (iv) Hazard function,  $b(t)$ ; (v) Probability of success,  $P_s$ ; (vi) Probability of failure,  $P_f$ ; (vii) Failure rate,  $\lambda$ ; (viii) Repair rate,  $\mu$ ; (ix) Mean time to failure, MTTF; (x) Mean time to repair, MTTR and (xi) Mean time between failure, MTBF.

The reliability is examined for SEIG rotor core for minimum excitation capacitor value. The failure of excitation involves, particularly for the SEIG generation failure. The failure of excitation is dealt primarily with the loss of SEIG operation. The reliability assessment of SEIG excitation through the capacitor is presented employing a minimal value of the excitation capacitor. Table 2 represents the estimated reliability indices.

### 5 | RESULTS AND DISCUSSION

The no-load characteristic of the SEIG is determined by synchronous speed test data as given in 'Appendix A'. The obtained



**TABLE 2** Evaluating the reliability related functions

Time interval	No. of failures in each interval	Cumul failures	No. of experiments	Failure density function	Cumul failure distribution	Survivor function	Hazard function
0	15	0	32	0.469	0.000	1.000	0.638
1	8	15	17	0.250	0.469	0.531	0.615
2	4	23	9	0.125	0.718	0.281	0.571
3	2	27	5	0.062	0.844	0.156	0.500
4	1	29	3	0.031	0.906	0.094	0.400
5	0	30	2	0.000	0.938	0.062	0.000
6	1	30	2	0.031	0.938	0.062	0.660
7	1	31	1	0.031	0.969	0.031	2.000

no-load characteristic of the experimental test machine is shown in Figure 4(a). In Figure 4(a), the points indicate the experimental results and the solid line represents the simulation results, which are obtained through routine plotting tool in MATLAB.

The magnetizing reactance  $X_m$  of the SEIG is considered as variable which depends on the core flux or the ratio of air-gap voltage to frequency ( $V_g/f$ ). Magnetization curve ( $V_g/F$  vs  $X_m$ ) of the SEIG is shown in Figure 4(b). This characteristic is evaluated from 'Appendix A' illustrations. The variation of  $X_m$  with  $V_g/f$  is non-linear due to magnetic saturation of the core [34].

In Figure 4(b), points indicate the experimental results and the solid line represents the simulation result, which is obtained through (2).

$$\frac{V_g}{f} = K_1 + K_2 X_m + K_3 X_m^2 + K_4 X_m^3; \text{ for } 70 \leq X_m \leq 130. \quad (2)$$

The least-square algorithm is employed to obtain the magnetization characteristic and the numerical-based routine curve tool is utilized in MATLAB to find the following coefficients of (2):

$$K_1 = 767.54, K_2 = -16.535, K_3 = -0.1843 \text{ and } K_4 = -7.46 \times 10^{-4}$$

## 5.1 | Self-excitation capacitance

The build-up of the terminal voltage for SEIG requires an excitation capacitor of minimum value. The minimum excitation capacitor value depends on speed,  $Z_L$ , and load power factor. The value of per phase capacitance is calculated at variable speed under the no-load condition as required in SEIG excitation. The capacitance value is determined experimentally to observe the voltage build-up and voltage collapse, as shown in Figure 4(c). This figure also shows that the capacitance value increases as the speed of the SEIG decreases [36, 37]. The minimum value of the capacitor is determined as 24.48  $\mu\text{F}$  at the synchronous speed of the SEIG. In Figure 4(c), points indicate the experimental results, and the solid line represents the mathematical simulation results.

## 5.2 | SEIG performance characteristics at variable rotor speed

Figures 5(a) and (b) show simulation and experimental values of the terminal voltage at different speeds for 36 and 40  $\mu\text{F}$  values of terminal capacitances, respectively. The curves are obtained under no-load condition as well as under a balanced resistive load (5.16 pu). The dashed line represents the resistive load for both figures. In Figures 5(a) and (b), points indicate the experimental results and the solid line represents the mathematical simulation result. The constant terminal voltage of pre-specified value is 220 V and the performance characteristics of the generator for 220 V are evaluated through Equations (5), (6) and (7) by putting the values  $\bar{Y}_{ab}$ ,  $\bar{Y}_{ac}$  and  $\bar{Y}_{ad}$  in Equation (3) and then distinguishing the real component and imaginary component, the two non-linear scalar equations X(1) and X(2) are obtained (refer Figure A1a).

$$\bar{Y}_{ab} + \bar{Y}_{ac} + \bar{Y}_{ad} = 0, \quad (3)$$

where

$$\bar{Y}_{ab} = \left[ \left( \frac{1}{\frac{R_L}{f} + jX_L} + \frac{1}{\frac{-jX_c}{f^2}} \right)^{-1} + \left( \frac{R_s}{f} + jX_s \right) \right]^{-1}, \quad (4a)$$

$$\bar{Y}_{ac} = \frac{1}{\frac{R_L}{f}} + \frac{1}{jX_m}, \quad (4b)$$

$$\bar{Y}_{ad} = \left[ \frac{R_r}{f - V} + jX_r \right]^{-1}, \quad (4c)$$

$$X(1) = \text{real}(\bar{Y}_{ab} + \bar{Y}_{ac} + \bar{Y}_{ad}) = 0, \quad (5)$$

$$X(2) = \text{imag}(\bar{Y}_{ab} + \bar{Y}_{ac} + \bar{Y}_{ad}) = 0, \quad (6)$$

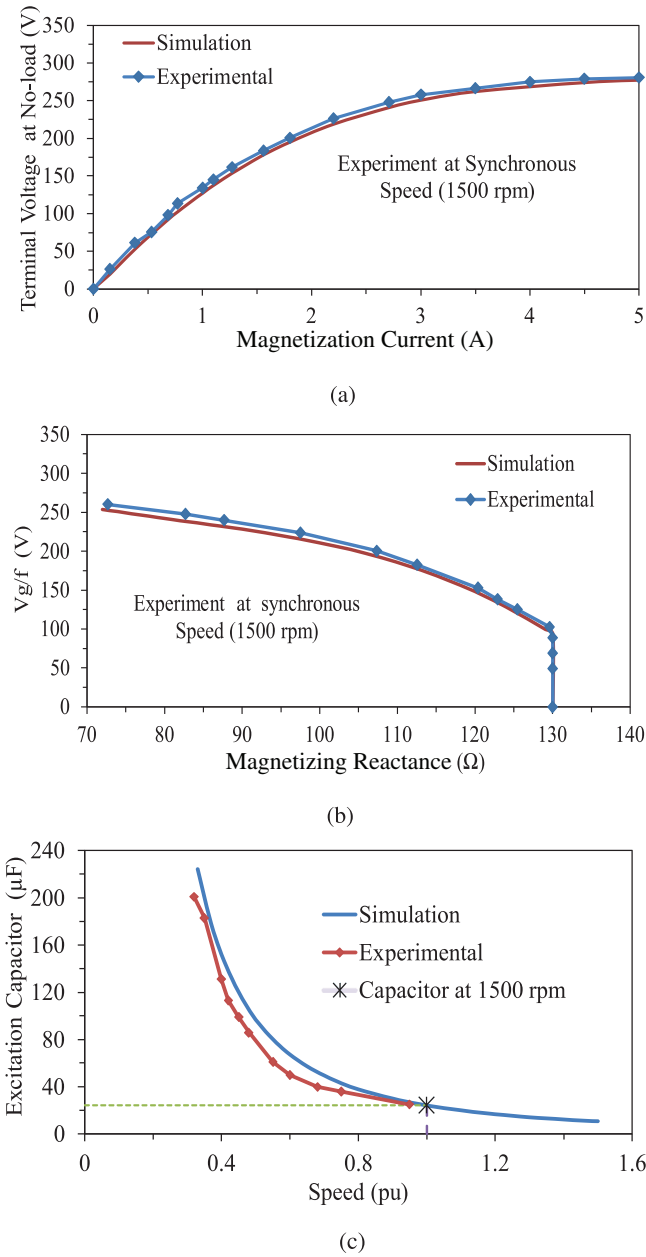


**FIGURE 4** (a) Variation of no-load voltage against magnetization current; (b) Magnetization characteristics of SEIG; (c) SEIG characteristics excitation capacitor with speed

$$X(3) = \left| \overline{V}_g \times \frac{\overline{Z}_{eb}}{\overline{Z}_{eb} + \overline{Z}_{ea}} \right| - V_t^{sp} = 0, \quad (7)$$

where

$$V_t = \left| \overline{V}_g \times \frac{\overline{Z}_{eb}}{\overline{Z}_{eb} + \overline{Z}_{ea}} \right|.$$

The maximum error occurred at the speed of 0.9 pu with 36  $\mu F$  in Figure 5(a). For this experiment, terminal voltage is obtained as 195 V. An equal terminal voltage is determined through

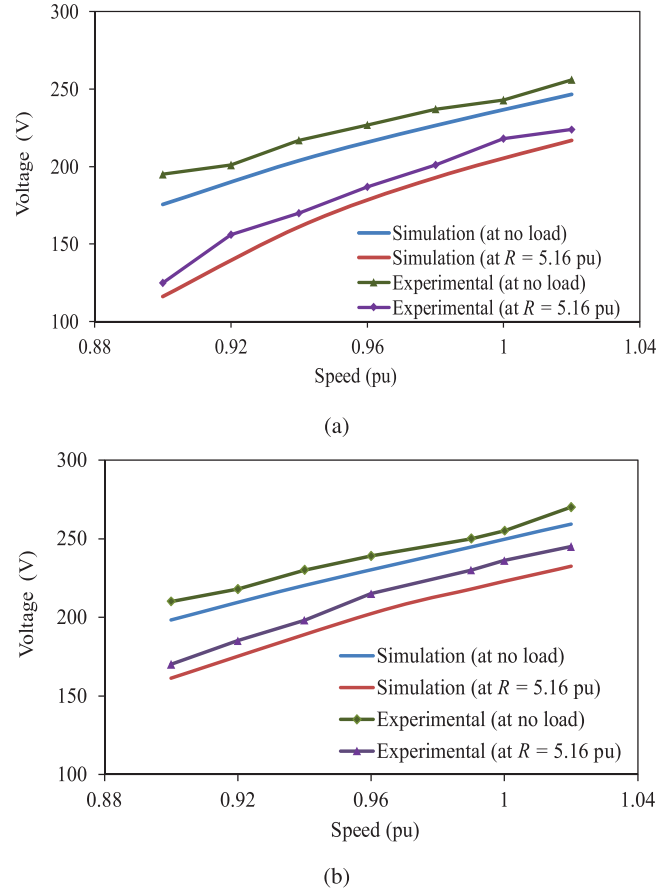


**FIGURE 5** SEIG characteristics with variable speed at (a) 36  $\mu F$ , (b) 40  $\mu F$

**TABLE 3** Variation in experimental and simulation-based excitation capacitor value at variable speed with 36  $\mu F$

S. No.	Voltage (V)	Experimental values		Speed (pu)	% error
		Cap. ( $\mu F$ )	Req. sim. cap. ( $\mu F$ )		
1	195	36	39.235	0.90	8.99
2	217	36	39.10	0.94	8.58
3	237	36	39.10	0.98	8.58
4	256	36	38.96	1.02	8.22

MATLAB simulation which requires a capacitor value of 39.235  $\mu F$ . It gives error in capacitor value required is 8.99%. As speed of the rotor increases this error decreases as shown in Table 3.

The maximum error occurred at the speed of 0.9 pu with 40  $\mu F$  in Figure 5(b). For this experiment, terminal voltage is obtained as 210 V. To find the equal terminal voltage through MATLAB simulation, a capacitor of 43.40  $\mu F$  is needed. It means the error is 8.5%. This error decreases with the increase in rotor speed as shown in Table 4. It can be also observed from Tables 3 and 4 that the error decreases with the increase in capacitor values.

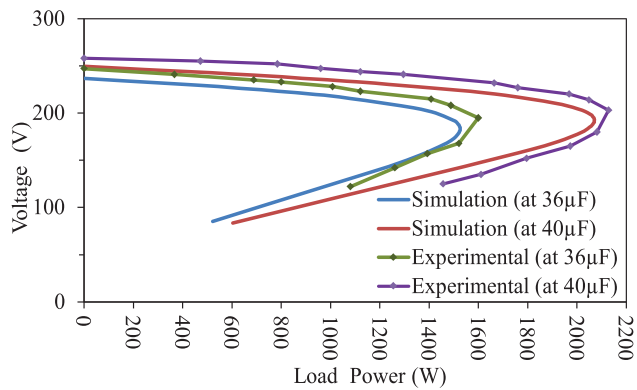
In Figures 6(a), (b), and (c), the points indicate the experimental results and the solid line represents the simulation results,

**TABLE 4** Variation in experimental and simulation-based excitation capacitor value at variable speed with 40  $\mu\text{F}$ 

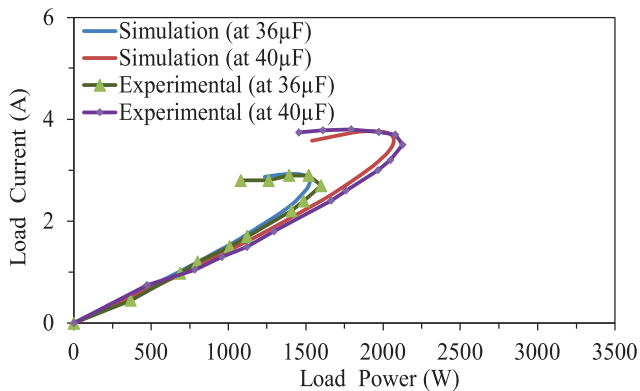
Experimental values				
S. No.	Voltage (V)	Cap. ( $\mu\text{F}$ )	Req. sim. cap. ( $\mu\text{F}$ )	Speed (pu)
1	210	40	43.40	0.90
2	229	40	43.15	0.94
3	253	40	43.00	0.99
4	267	40	42.60	1.02

**TABLE 5** Variation in experimental and simulation-based excitation capacitor value at constant speed with 36  $\mu\text{F}$ 

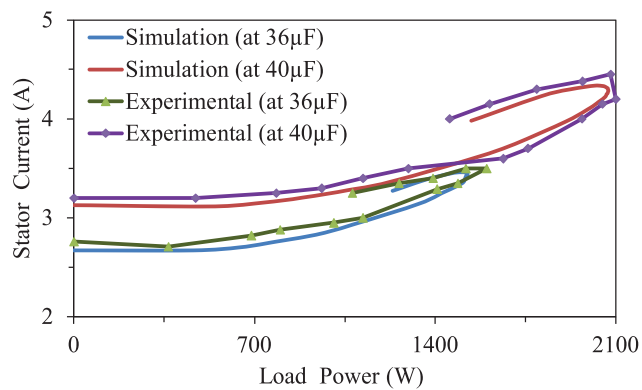
Experimental values		Simulation values		
S. No.	Voltage (V)	Cap. ( $\mu\text{F}$ )	Req. cap. ( $\mu\text{F}$ )	% error
1	246	36	39.06	8.50
2	232	36	38.40	6.66
3	223	36	37.59	4.42
4	208	36	37.12	3.11



(a)



(b)



(c)

**FIGURE 6** SEIG load characteristics with variable excitation capacitor at 36 and 40  $\mu\text{F}$ . (a) Terminal voltage versus load power, (b) Load current versus load power, (c) Stator current versus load power**TABLE 6** Variation in experimental and simulation-based excitation capacitor value at constant speed with 40  $\mu\text{F}$ 

Experimental values			Simulation values	
S. No.	Voltage (V)	Cap. ( $\mu\text{F}$ )	Req. cap. ( $\mu\text{F}$ )	% error
1	260	40	43.00	7.50
2	247	40	42.90	7.25
3	232	40	42.87	7.175
4	220	40	42.00	5.00

which can be obtained through (5) and (6). Figure 6(a) shows the simulation and experiment results of terminal voltage versus output power  $P_o$  characteristic of the SEIG at different values of excitation capacitors (36 and 40  $\mu\text{F}$ ) at synchronous speed ( $V = 1$  pu). Tables 5 and 6 show the percentage error of 36 and 40  $\mu\text{F}$ , respectively, under load condition with a constant rotor speed. The error in the highest power is determined for 36 and 40  $\mu\text{F}$  capacitance. The error found for 36 and 40  $\mu\text{F}$  capacitors are 5.57%, and 2.80%, respectively. The highest electrical power is attained as 1.610 and 2.128 kW experimentally for 36 and 40  $\mu\text{F}$ , respectively. To achieve a comparable maximum power with the aid of simulation, 36.624  $\mu\text{F}$  is required for 1.610 kW and 40.454  $\mu\text{F}$  is required for 2.128 kW. It signifies that the error in the excitation capacitor is 1.73% and 1.13%, respectively, which are within the tolerance limit of capacitor utilized, i.e. 5%. The error in peak power has also been assessed.

The percentage error in output voltage of the generator for 36 and 40  $\mu\text{F}$  capacitors are found in Tables 5 and 6, respectively. To obtain the same voltage in simulation, the required values of a capacitor (required simulation capacitance) are shown in Tables 5 and 6. It is obvious from the table that under the normal operating region, the error decreases with the decrease in voltage.

Figure 6(b) shows the load characteristics (load current ( $I_L$ ) vs.  $P_o$ ) of the generator at 36 and 40  $\mu\text{F}$  excitation capacitors. In these characteristics, at  $Z_L$  is less than  $\infty$  (at zero loading condition), initially both the  $P_o$  and  $I_L$  increases from zero, and this represents the normal operating region. This region continues until the maximum  $P_o$  point  $P_{\max}$  is reached. After  $P_{\max}$  point, reduction in  $Z_L$  results in a decrease in both the  $P_o$  and  $I_L$ , until the critical  $Z_L$  is reached and the loss of excitation occurs of the

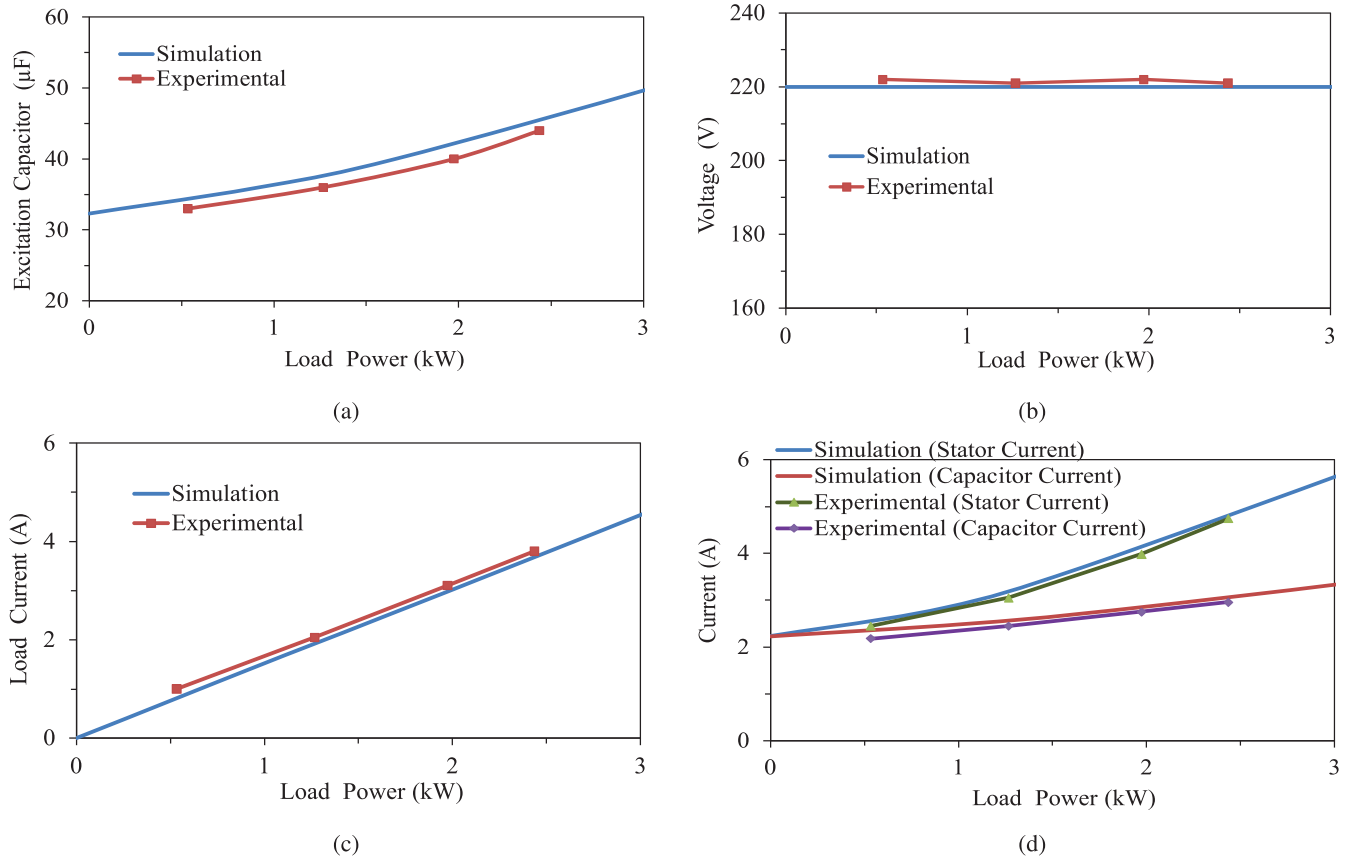


**FIGURE 7** Constant terminal voltage ( $V = 1$  pu) characteristics of SEIG with load power. (a) Excitation capacitor versus load power, (b) Voltage versus load power, (c) Load current versus load power, (d) Stator current versus load power

generator, which represents the abnormal region of operation [34].

Figure 6(c) shows the load characteristics (stator current ( $I_S$ ) vs.  $P_0$ ) of the generator at 36 and 40 μF excitation capacitors. The  $I_S$  is noticed to be highly inconsiderate to  $Z_L$  and considerate to  $X_C$ . It is because of  $I_S$ , which is the phasor summation of  $I_L$  and  $I_C$ . In this situation, the reduction of  $I_C$  is partly taken care of by increasing  $I_L$ , and this is why  $I_S$  continues to be constant. At maximum power, the value of  $I_S$  is either greater or lesser than its constant value; this is why it depends on the constant parameter of the SEIG.

The constant terminal voltage of pre-specified value is 220 V and the performance characteristics of the generator for 220 V are evaluated through (5), (6) and (7). In this case, find the values of  $X_m$ ,  $F$ , and  $X_C$  for given various possible values of  $Z_L$  and a fixed value of  $V$  [34, 38].

The variation of excitation capacitor, voltages, load current and stator/capacitor currents against output/load power  $P_0$  are shown in Figures 7(a), (b), (c) and (d), respectively. To maintain a constant terminal voltage, more capacitors are required. Due to this, the  $Z_L$  is reduced and hence  $I_C$  is increased. The  $I_L$  increases linearly with  $P_0$  as the terminal voltage is constant. In this phenomena, both  $I_L$  and  $I_C$  increase and therefore the  $I_S$  increases with  $P_0$ . The critical characteristics cannot

be found only by using Figures 4(a) and (b) and (2). The graph and equation do not have adequate information to be solved. In Figure 4(b), the value of  $X_m$  is in the range from 70 to 130 Ω. If  $X_m$  is decreased below the lower value of the above range, the earlier (2) still needs considerable algebraic manipulation for being solved. The equations are as follow:

$$\frac{V_g}{f} = K_5 + K_6 X_m; \text{ for } 60 \leq X_m \leq 70, \quad (8)$$

$$\frac{V_g}{f} \approx 272; \text{ for } X_m \leq 60. \quad (9)$$

The coefficients of (2) and (8) are as:

$$K_1 = 767.54, K_2 = -16.535, K_3 = -0.1843, K_4 = -7.46 \times 10^{-4}, K_5 = 316.15, K_6 = -0.82$$

Figure 8(a) shows the critical characteristics of SEIG (excitation capacitor vs. load resistance) at synchronous speed. To operate the SEIG within its design specifications, it is necessary to keep  $I_S$  as close as possible to the designed limit. So the SEIG performance characteristics are determined at a specified  $I_S$ , which increases with capacitor values. When the capacitor value is reached on 140 μF, then the generator gives 12.5 A stator current. Thus, the obtained value of

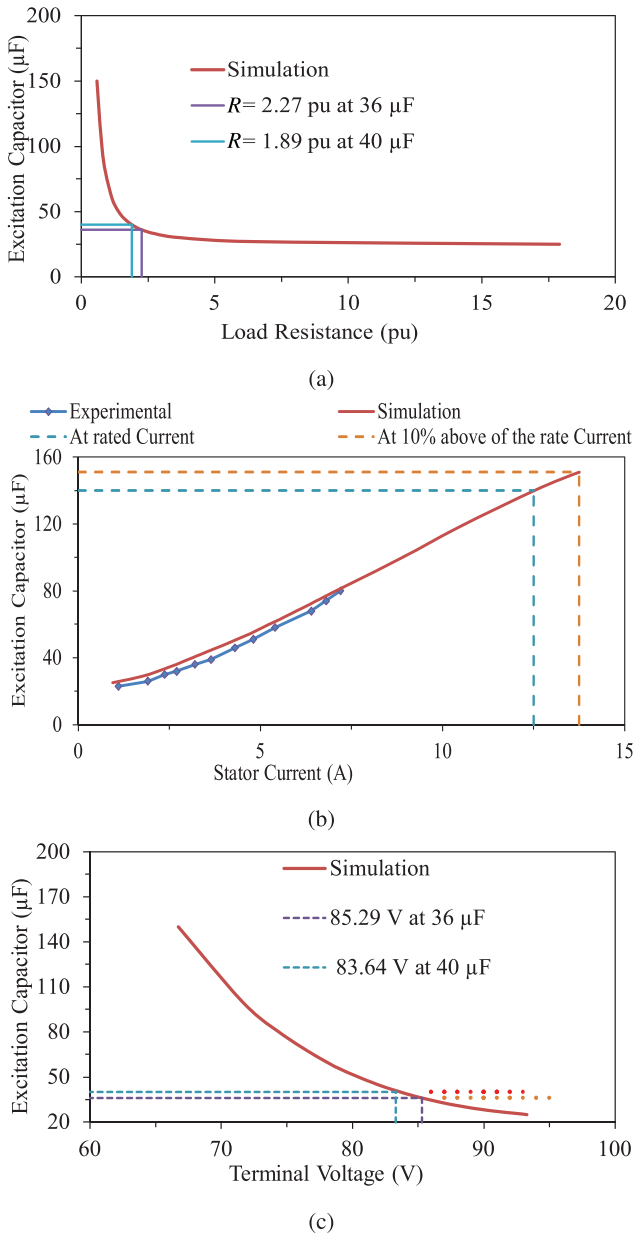


**FIGURE 8** Critical characteristics of SEIG on excitation capacitor with (a) Stator current, (b) Load resistance and (c) Terminal voltage

capacitor is called the critical capacitor for this generator. Figures 8(a), (b) and (c) show the critical characteristics of SEIG on excitation capacitor versus terminal voltage and excitation capacitor versus load resistance (pu), respectively. In the abnormal region (with more reduction in  $Z_L$ ) both  $P_O$  and  $I_L$  decrease until the critical  $Z_L$  is reached and loss of self-excitation occurs in the generator. These figures give the information about the critical resistance value and critical voltage for a particular capacitor at a fixed speed (synchronous speed), where the loss of excitation occurs in the generator after these critical values. These critical values are obtained experimentally, which is not so easy. Thus, the experimental result for 36 and  $40 \mu\text{F}$  of critical voltage is in range (87 V, 95 V) and (86 V, 92 V), respectively.

### 5.3 | Reliability function evaluation for SEIG

The PDFs are employed to illustrate the RE of SEIG excitation. Authors have performed 32 laboratory experiments on Day 1. All experiments are carried out by raising the reactive load. Now on Day 2, the overall number of experiments is equal to the Day 1 experiments minus total failures arising preceding time spell. The experimental data are collected for seven intervals. Using the above experimental results, the reliability indices like  $f(t)$ ,  $F(t)$ ,  $f_s(t)$  and  $b(t)$  are arranged in Table 2.

The assessment of reliability indices are done employing the following steps:

- (i) Compute the overall number of failures in each time spell of Day 1,
- (ii) Evaluate the reliability indices  $f(t)$ ,  $F(t)$ ,  $f_s(t)$  and  $b(t)$ .

All reliability indices  $f(t)$ ,  $F(t)$ ,  $f_s(t)$  and  $b(t)$  are explained graphically in Figures 9(a), (b), (c) and (d), respectively. Table 2 is described as follows:

- (i) Time interval in the number of days are chosen as one,
- (ii) Number of failures are examined experimentally,
- (iii) Cumulative failures are the summation of failures in each interval,
- (iv) The overall number of experiments on next days is matched to the day before experiments minus all the failures occurred in the previous time interval,
- (v)  $f(t)$  = (number of failures during a time interval)/32,
- (vi)  $F(t)$  = (cumulative number of failures)/32,
- (vii)  $f_s(t)$  = (cumulative number of survivors)/32,
- (viii)  $b(t)$  = (number of failures in time spell)/(mean number of a survivor for that period).

The laboratory experiment is done considering the minimum capacitance value, i.e.  $25 \mu\text{F}$ . The success and failure of the performed experiment are dependent on the chance of SEIG excitation failure. The experiment is performed for 71 times within seven spell or eight days and reliability is assessed using Monte-Carlo method. The experimental results in terms of success and failure of SEIG excitation are shown in Table 7.

The simulation parameters, namely, success probability and failure probability are shown in Figures 10(a) and (b). These simulation results conferred that

- (i)  $P_s$  and  $P_f$  has better values when the experiment on SEIG excitation is repeated in large number;
- (ii) The actual value of  $P_s$  and  $P_f$  fluctuates post experimental tests. Therefore, the average value of  $P_s$  and  $P_f$  cannot be treated as true value;
- (iii) If the number of experiments is raised, the  $P_s$  and  $P_f$  values tend to achieve the actual value;
- (iv) The value of  $P_s$  is 0.55 and  $P_f$  is 0.45 in the simulation results.  $P_s$  and  $P_f$  are analytically evaluated as given in (10) and (11), respectively.



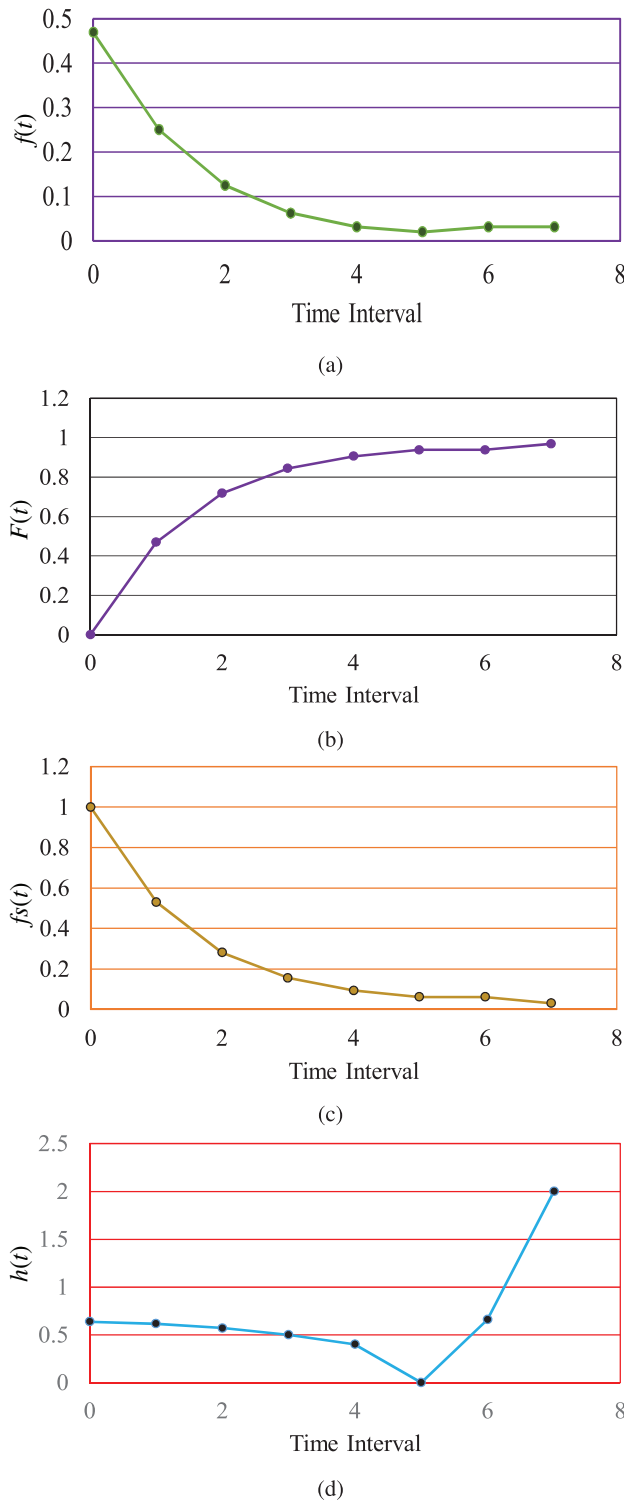


**FIGURE 9** Reliability evaluation functions: (a)  $f(t)$  curve, (b)  $F(t)$  curve, (c)  $f_s(t)$  curve and (d)  $h(t)$  curve

$$P_s = \frac{S}{T} = \frac{39}{71} = 0.5490, \quad (10)$$

$$P_f = \frac{F}{T} = \frac{32}{71} = 0.4510, \quad (11)$$

**TABLE 7** Evaluating the reliability related functions considering excitation failure

No. of experiments	Outcome of experiments	Probability of	
		Success (S)	Failure (F)
1	S	1	0
2	S	1	0
3	F	0.67	0.33
4	S	0.75	0.25
5	F	0.60	0.40
6	S	0.67	0.33
7	F	0.57	0.43
67	S	0.55	0.45
68	S	0.56	0.44
69	F	0.55	0.45
70	S	0.56	0.44
71	F	0.55	0.45

where  $T$  is number of possible outcomes,  $S$  is number of success and  $F$  is number of failures. In Municipal wastewater-based Micro-hydro power generation system, reliability data and other parameters are illustrated and SEIG is used for power generation [31].

The RE of SEIG is further extended considering the variable wind speeds. The SEIG is proficient in wind power application during different wind speeds. Thus, it is required to assess the reliability of SEIG for different wind speeds. Therefore, random wind speed data is generated between 5 and 25 m/s, as illustrated in Table 8. So, a correlation between wind speed and rotor speed is required to be established, which is described in Equations (A13)–(A15) of Appendix A.4. The following assumptions are considered while formulating the correlation:

- Diameter of the wind turbine rotor blade is 60 m.
- Gear-box gear ratio is 50:1.
- Tip speed ratio is 7.
- SEIG has a constant average failure rate.

The optimal wind speed is obtained as 13.428 m/s for rotor speed of SEIG to be greater than synchronous speed for power generation. Thus, the wind speeds lesser than the optimal wind speed considered as failure condition of the SEIG. As seen from Figure 11, a constant average failure rate is calculated and the SEIG reliability is obtained as an exponential function. The reliability is then compared for 0.2 and 0.3 failure rates, respectively. It is observed from the waveforms that the SEIG operation is reliable for wind speeds higher than 13.428 m/s and the SEIG reliability is better if failure rates are smaller.

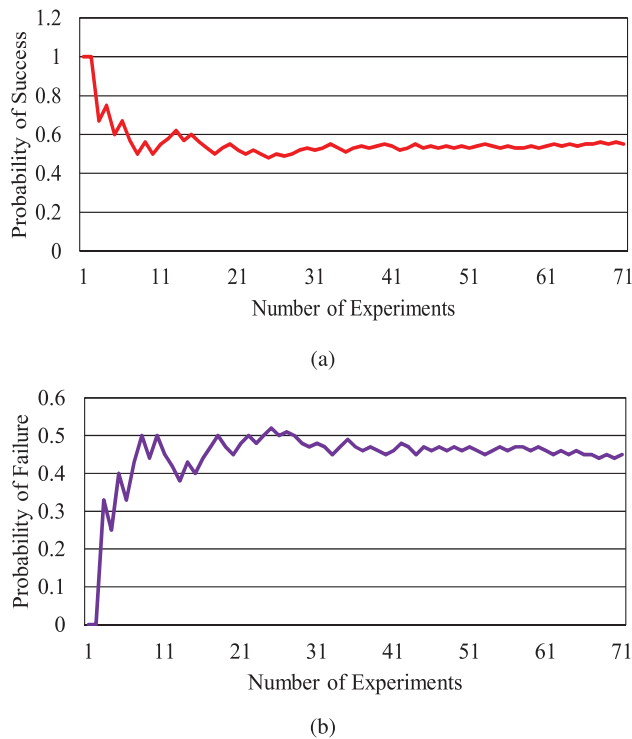


**FIGURE 10** Reliability evaluation using Monte-Carlo simulation: (a) Probability of success, (b) Probability of failure

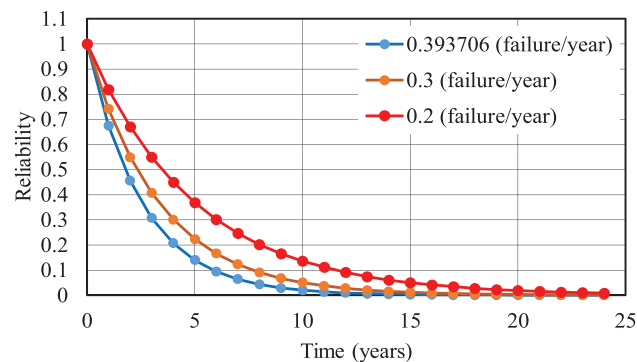


**FIGURE 11** Reliability evaluation of SEIG under different wind speeds

## 6 | CONCLUSION AND SCOPES FOR THE FUTURE WORK

The research work includes the performance and RE of 3- $\phi$  induction machine, working as a SEIG. The SEIG is very popular in remote areas (of a country like India where the power grid is not accessible) for power generation using conventional and non-conventional energy resources. However, designed SEIG is under consideration, neither economical nor easily available in the market. Thus, the induction machine has been utilized as a SEIG with the proper value of the capacitor.

A 3- $\phi$  induction machine coupled with DC shunt motor has been demonstrated as SEIG in the Department of Electrical Engineering, IIT(BHU), Varanasi, India, Electrical Machine lab-

**TABLE 8** Evaluating the reliability function under different wind speeds

S. No.	Wind (m/s)	Success or Failure	Probability of	
			Success (S)	Failure (F)
1	22.5	S	1	0
2	21.5	S	1	0
3	15	S	1	0
4	7	F	0.75	0.25
5	5	F	0.6	0.40
6	14.5	S	0.67	0.33
7	18	S	0.72	0.28
96	22.5	S	0.573	0.427
97	16.5	S	0.577	0.423
98	6	F	0.57	0.43
99	5.5	F	0.565	0.435
100	13	F	0.56	0.44
Average Failure Rate			0.393706	

oratory with variable resistive loads at constant shaft speed and constant load at variable shaft speed. The no-load characteristic of the machine is determined to evaluate the minimum capacitance at synchronous speed. Hence, the performance of the SEIG is depicted. The minimum capacitor value obtained experimentally is 24.48  $\mu$ F at synchronous speed. The experiments are performed with 25  $\mu$ F, which is very close to the 24.48  $\mu$ F. All experiments, including on load and no-load conditions at variable speed and synchronous speed are performed, and several characteristics are obtained. These characteristics are found almost similar in comparison to its original pattern. The percentage error between experimental results and simulation results using 36 and 40  $\mu$ F capacitors at no load condition with variable speed and on load condition with the speed of the SEIG were determined. The errors in the maximum power were determined for 36 and 40  $\mu$ F capacitors as 5.57% and 2.80%, respectively. The errors in the capacitor value are obtained as 1.73% and 1.13%, respectively, when the same maximum power in simulation is obtained.

The critical performance and RE of the SEIG were obtained using the required minimum capacitance for the successful operation. The critical value of capacitance was found 140  $\mu$ F. Dealing with these prospects, the reliability estimation of RM in the rotor iron core of the SEIG has been carried out utilizing a possibility distribution approach and the Monte-Carlo approach. The obtained values are 0.5490 and 0.4510 for  $P_s$  and  $P_f$ , respectively. These values are obtained by implementing the Monte-Carlo method that tends towards 0.55 and 0.45 for  $P_s$  and  $P_f$ , respectively. Both numerical and simulation results are identified to be approximately the same. The curves for the

functions  $f(t)$ ,  $F(t)$ ,  $f_s(t)$  and  $b(t)$  of the 3- $\phi$  induction machine working as a SEIG have been obtained. Furthermore, reliability has been evaluated for SEIG under different wind speeds. It is found that the wind speed has a correlation with SEIG rotor speed, which aids in obtaining the reliability function. The average constant failure rate of 0.393706 was obtained considering different wind speed data. The reliability of SEIG has been improved for lower values of failure rates, and SEIG faces lesser failures for speeds higher than 13.428 m/s.

The summary of the accomplished work is as follows:

- (i) Rated  $I_s$  gives information about the maximum limit of the capacitor for the safe performance of SEIG.
- (ii) Reduction in percentage error indicates the point where the successful performance and reliability of the three-phase induction machine operated as SEIG is high at the particular capacitor value, shaft speed and variable load resistance.
- (iii) Critical performance of SEIG is required for stable power generation.
- (iv) Reliability indices including  $f(t)$ ,  $F(t)$ ,  $f_s(t)$  and  $b(t)$  are evaluated experimentally for RE of SEIG. Also, the reliability of SEIG has been evaluated at different wind speeds.
- (v) The experimentally evaluated area under failure density curve is one, which is similar to the theoretical approach.
- (vi) Success and failure probabilities of three-phase squirrel cage induction machine operated as SEIG are obtained experimentally. The evaluated numerical values were 0.5490 and 0.4510, respectively.

The work presented can be extended with FACTS devices like STATCOM for compensating  $Q$  during SEIG isolated or grid-connected mode of operations. Researchers can study the effect of impedance loading on SEIG performance in the wind energy conversion system (WECS) as future work. The SEIG performance can be compared with other WECS-based generators. Also, an ELC can be used to regulate frequency and voltage in their limits.

## NOMENCLATURE

$\angle\theta$	Load Power Factor
$\lambda$	Failure Rate
$\mu$	Repair Rate
$\phi$	Power Factor Angle
$C_{\max}$	Capacitor maximum value
$C_{\min}$	Capacitor minimum value
$f$	Frequency
$F(t)$	Cumulative Distribution Function
$f(t)$	Probability Distribution Function
$f_s(t)$	Survivor Function
$FR$	Frequency Regulation
$b(t)$	Hazard Rate
$I_C$	Capacitive Current
$I_L$	Load Current
$I_s$	Stator Current
$IG$	Induction Generator
$IM$	Induction Motor

$MTBF$	Mean Time Between Failure
$MTTF$	Mean Time To Failure
$MTTR$	Mean Time To Repair
$P_f$	Failure Probability
$P_O$	Output Power
$P_s$	Success Probability
$Q$	Reactive Power
$R_c$	Core Resistance
$X_L$	Load Reactance
$X_r$	Rotor Reactance
$X_s$	Stator Reactance
$RE$	Reliability Evaluation
$S$	Apparent Power
$SEIG$	Self-Excited Induction Generator
$v$	Rotor Speed
$VR$	Voltage Regulation
$WECS$	Wind Energy Conversion System
$X_c$	Excitation Capacitance
$R_L$	Load Resistance
$X_m$	Magnetizing Reactance
$R_r$	Rotor Resistance
$R_s$	Stator Resistance
$Y_{ab}, Y_{ac}, Y_{ad}$	Equivalent Terminal Admittances
$Z_L$	Load Impedance
$Z_{ac}, Z_{bc}$	Equivalent Terminal Impedances
$V_g$	Air Gap Voltage
$V_i \text{ or } V$	Terminal Voltage
$V_i^{sp}$	Pre-specified Terminal Voltage

## ACKNOWLEDGEMENT

The authors whole heartily thank the Department of Electrical Engineering, Indian Institute of Technology (Banaras Hindu University), Varanasi for providing the laboratory related facilities to accomplish the research work in time.

## ORCID

Sachin Kumar  <https://orcid.org/0000-0003-1517-7450>

R.K. Saket  <https://orcid.org/0000-0002-2773-9599>

## REFERENCES

- Kumar, S.S., et al.: Modelling, analysis and control of stand-alone self-excited induction generator-pulse width modulation rectifier systems feeding constant DC voltage applications. IET Gener. Transm. Distrib. 8(6), 1140–1155 (2014)
- Arthishri, K., et al.: Simplified methods for the analysis of self-excited induction generators. IET Electr. Power Appl. 11(9), 1636–1644 (2017)
- Li, H., et al.: Build-up steady-state analysis of wind-driven self-excited induction generators. J. Eng. 2017(13), 1383–1387 (2017)
- Chauhan, Y.K., et al.: Optimum utilisation of self-excited induction generator. IET Electr. Power Appl. 7(9), 680–692 (2013)
- Vanço, W.E., et al.: A proposal of expansion and implementation in isolated generation systems using self-excited induction generator with synchronous generator. IEEE Access 7, 117,188–117,195 (2019)
- Ammasaigounden, N., Subbiah, M., Krishnamurthy, M.: Wind-driven self-excited pole-changing induction generators. IEE Proc. B Electr. Power Appl. 133(5), 315–321 (1986)
- Wang, L., Lee, C.-H.: A novel analysis on the performance of an isolated self-excited induction generator. IEEE Trans. Energy Convers. 12(2), 109–117 (1997)

8. Raj, R.E., Kamalakannan, C., Karthigaivel, R.: Genetic algorithm-based analysis of wind-driven parallel operated self-excited induction generators supplying isolated loads. *IET Renewable Power Gener.* 12(4), 472–483 (2017)
9. Singh, G.: Self-excited induction generator research—A survey. *Electr. Power Syst. Res.* 69(2-3), 107–114 (2004)
10. Shridhar, L., Singh, B., Jha, C.: A step towards improvements in the characteristics of self excited induction generator. *IEEE Trans. Energy Convers.* 8(1), 40–46 (1993)
11. Wang, L., Deng, R.-Y.: Transient performance of an isolated induction generator under unbalanced excitation capacitors. *IEEE Trans. Energy Convers.* 14(4), 887–893 (1999)
12. Teng, K., et al.: Voltage build-up analysis of self-excited induction generator with multi-timescale reduced-order model. *IEEE Access* 7, 48,003–48,012 (2019)
13. Wang, L., Lee, C.-H.: Long-shunt and short-shunt connections on dynamic performance of a SEIG feeding an induction motor load. *IEEE Trans. Energy Convers.* 15(1), 1–7 (2000)
14. Singh, B., Singh, M., Tandon, A.: Transient performance of series-compensated three-phase self-excited induction generator feeding dynamic loads. *IEEE Trans. Ind. Appl.* 46(4), 1271–1280 (2010)
15. Chilipi, R.R., et al.: Design and implementation of dynamic electronic load controller for three-phase self-excited induction generator in remote small-hydro power generation. *IET Renewable Power Gener.* 8(3), 269–280 (2014)
16. Gao, S., et al.: Efficient voltage regulation scheme for three-phase self-excited induction generator feeding single-phase load in remote locations. *IET Renewable Power Gener.* 8(2), 100–108 (2013)
17. Thakur, R., Agarwal, V.: Application of interval computation technique to fixed speed wind energy conversion system. In: *IEEE International Conference on Sustainable Energy Technologies*, pp. 1093–1098. IEEE, (2008)
18. Singh, B., et al.: Static synchronous compensator-variable frequency drive for voltage and frequency control of small-hydro driven self-excited induction generators system. *IET Gener. Transm. Distrib.* 8(9), 1528–1538 (2014)
19. Singh, B., et al.: Implementation of modified current synchronous detection method for voltage control of self-excited induction generator. *IET Power Electron.* 8(7), 1146–1155 (2015)
20. Scherer, L.G., Tambara, R.V., de Camargo, R.F.: Voltage and frequency regulation of standalone self-excited induction generator for micro-hydro power generation using discrete-time adaptive control. *IET Renewable Power Gener.* 10(4), 531–540 (2016)
21. Tischer, C.B., et al.: Proportional-resonant control applied on voltage regulation of standalone SEIG for micro-hydro power generation. *IET Renewable Power Gener.* 11(5), 593–602 (2017)
22. Kalla, U.K., Singh, B., Murthy, S.S.: Slide mode control of microgrid using small hydro driven single-phase SEIG integrated with solar PV array. *IET Renewable Power Gener.* 11(11), 1464–1472 (2017)
23. Aoyama, M., Noguchi, T., Motohashi, Y.: Proposal of self-excited wound-field magnetic-modulated dual-axis motor for hybrid electric vehicle applications. *IET Electr. Power Appl.* 12(2), 153–160 (2017)
24. Vanco, W.E., et al.: Experimental analysis of a self-excited induction generators operating in parallel with synchronous generators applied to isolated load generation. *IEEE Lat. Am. Trans.* 14(4), 1730–1736 (2016)
25. Jordan, R.K., et al.: Novel solutions for high-speed self-excited induction generators. *IEEE Trans. Ind. Electron.* 63(4), 2124–2132 (2015)
26. Kumar, S., et al.: Reliability enhancement of electrical power system including impacts of renewable energy sources: A comprehensive review. *IET Gener. Transm. Distrib.* 14(10), 1799–1815 (2020)
27. Ramirez, J.M., Torres, M.E.: An electronic load controller for self-excited induction generators. In: *IEEE Power Engineering Society General Meeting*, pp. 1–8. IEEE, (2007)
28. Saket, R.: Reliability evaluation of defence support systems. In: Jain, L.C., Aidman, E.V., Abeynayake, C. (eds). *Innovations in Defence Support Systems-2*, pp. 241–286. Springer, Berlin (2011)
29. Arya, L., Choube, S., Saket, R.: Generation system adequacy evaluation using probability theory. *J. Inst. Eng. (India) Electr. Eng. Div.* 81(4), 170–174 (2001)
30. Saket, R., Bansal, R.C., Singh, G.: Reliability evaluation of power system considering voltage stability and continuation power flow. *J. Electr. Syst.* 3(2), 48–60 (2007)
31. Saket, R.: Design aspects and probabilistic approach for generation reliability evaluation of MWW based micro-hydro power plant. *Renewable Sustainable Energy Rev.* 28, 917–929 (2013)
32. Saket, R., Bansal, R.C., Kumar, K.A.: Reliability evaluation of micro hydro-photo-voltaic hybrid power generation using municipal waste water. *GMSARN Int. J.* 1, 13–20 (2007)
33. Bansal, R.: Three-phase self-excited induction generators: An overview. *IEEE Trans. Energy Convers.* 20(2), 292–299 (2005)
34. Haque, M.: A novel method of evaluating performance characteristics of a self-excited induction generator. *IEEE Trans. Energy Convers.* 24(2), 358–365 (2009)
35. Haque, M.: Self-excited single-phase and three-phase induction generators in remote areas. In: *International Conference on Electrical and Computer Engineering*, pp. 38–42. IEEE, (2008)
36. Eltamaly, A.M.: New formula to determine the minimum capacitance required for self-excited induction generator. In: *Proceedings of IEEE 33rd Annual IEEE Power Electronics Specialists Conference (Cat. No. 02CH37289)*, vol. 1, pp. 106–110. IEEE (2002)
37. Shridhar, L., et al.: Selection of capacitors for the self regulated short shunt self excited induction generator. *IEEE Trans. Energy Convers.* 10(1), 10–17 (1995)
38. Joshi, D., Sandhu, K.S., Soni, M.K.: Constant voltage constant frequency operation for a self-excited induction generator. *IEEE Trans. Energy Convers.* 21(1), 228–234 (2006)

**How to cite this article:** Varshney L, Vardhan AS, Vardhan AS, Kumar S, Saket RK, Sanjeevikumar P. Performance characteristics and reliability assessment of self-excited induction generator for wind power generation. *IET Renew. Power Gener.* 2021;15:1927–1942. <https://doi.org/10.1049/rpg2.12116>

## APPENDIX A

### A.1 | No-load test

The input  $S$ ,  $Q$  and  $\phi$  of the self-excited induction generator (SEIG) is obtained by (A1), (A2) and (A3).

$$S = \sqrt{3}VI, \quad (\text{A1})$$

$$Q = \sqrt{S^2 - P^2}, \quad (\text{A2})$$

$$\phi = \arctan\left(\frac{Q}{P}\right), \quad (\text{A3})$$

air gap voltage ( $V_g$ )

$$= \text{mod} [V' - I'(\cos \phi - j \sin \phi)(R_r + jX_r)], \quad (\text{A4})$$

where  $V'$  is calculated phase voltage,  $I'$  is calculated phase current of SEIG, respectively. The values of  $R_r$  and  $X_m$  are described by (A5), (A6) which are obtained from  $P$  and  $Q$  power

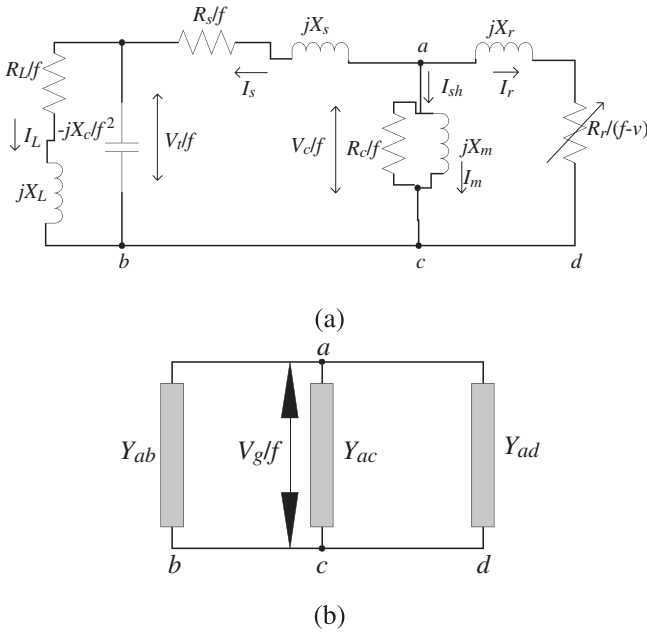


**FIGURE A1** (a) The per-phase equivalent circuit of three-phase SEIG; (b) Nodal admittance approach circuit of Figure 12(a) is represented by the three parallel impedances

balance equations.

$$R_c = \frac{V_g^2}{P - 3I_1^2 R_s}, \quad (\text{A5})$$

$$X_m = \frac{V_g^2}{Q - 3I_1^2 X_s}. \quad (\text{A6})$$

The  $R_c$  value is recognized as the average of all numerical values established from (A5). The average value of  $R_c$  is 1.48527 k $\Omega$ .

### A.2 | Performance characteristics equations

$X_m$  is obtained and  $V_g/f$  can be evaluated from (2) using  $X_m$ . The voltage, current and power are described by (A7)–(A12).

$$I_s = \frac{V_g}{f} Y_{bc}, \quad (\text{A7})$$

$$\frac{V_t}{f} = \frac{V_g}{f} - I_s Z_{ac}, \quad (\text{A8})$$

$$I_c = \frac{V_{ab}}{\frac{-jX_c}{F^2}}, \quad (\text{A9})$$

$$\bar{I}_C = \frac{\frac{\bar{V}_t}{f}}{\frac{-jX_c}{f^2}}, \quad (\text{A10})$$

$$\bar{I}_L = \frac{\frac{\bar{V}_t}{f}}{\frac{R_L}{f} + jX_L}, \quad (\text{A11})$$

$$P_L = 3 |I_L|^2 |R_L|. \quad (\text{A12})$$

### A.3 | Use of experimental equipment

(i) 0–750 AC/DC Wattmeter 10/20 A or 5/10 A, (ii) 0–10/20 A or 5/10 A, 50 Hz, AC Ammeter, (iii) 0–300/600 V, 50 Hz, AC Voltmeter, (iv) Tachometer, (v) 36  $\mu\text{F} \pm 5\%$ , 440 V AC, 50 Hz, Capacitor, (vi) Two-Way Switch, (vii) DPDT (double-pole double-throw), (viii) Rheostat, (ix) 0–290  $\Omega$ , 1.5 A, (x) 0–100  $\Omega$ , 5 A, (xi) 0–25  $\Omega$ , 25 A.

### A.4 | Equations related to reliability evaluation (RE) of SEIG under different wind speeds

$$\frac{\text{Wind turbine rotor blade speed}}{\text{SEIG rotor speed}} = \frac{50}{1} = \text{Gear Ratio} \quad (\text{A13})$$

$$\text{Wind turbine rotor tip speed; } S \text{ (mph)} = 0.0372 \times \pi \times D \times \omega \quad (\text{A14})$$

where  $D$  is diameter of wind turbine rotor blade,  $\omega$  is rotational speed of wind turbine rotor blade.

$$\text{Wind speed (m/s)} = 0.44704 \times \frac{S}{7}. \quad (\text{A15})$$